

DEEPLY VIRTUAL PSEUDOSCALAR MESON PRODUCTION WITH CLAS

V. Kubarovsky^{1,2,†}, P. Stoler² and I. Bedlinsky³

¹*Jefferson Lab, Newport News, USA,*

²*Rensselaer Polytechnic Institute, Troy, USA,*

³*Institute for Theoretical and Experimental Physics, Moscow, Russia*

[†]*Email: vpk@jlab.org*

Introduction.

Deeply virtual exclusive reactions offer a unique opportunity to study the structure of the nucleon at the parton level as one varies both the size of the probe, i.e. the photon virtuality Q^2 , and the momentum transfer to the nucleon t . Such processes can reveal much more information about the structure of the nucleon than either inclusive electroproduction (Q^2 only) or elastic form factors ($t = -Q^2$). The characterization of deeply virtual exclusive reactions in terms of their common nucleon structure is one of the major objectives of the Jefferson Lab 12 GeV upgrade.

There have been two commonly used theoretical tools which relate exclusive reactions to the structure of the nucleon. At lower Q^2 , where the probe is on the order of the size of hadrons and the interactions are strong, Regge phenomena have proved effective. At high Q^2 the probe interacts with individual quarks, and in the limit $Q^2 \rightarrow \infty$ and $-t/Q^2 \rightarrow 0$ the QCD factorization theorem [1] unifies all exclusive reactions in terms of their common nucleon structure encoded by generalized parton distributions (GPDs). In this article we consider deeply virtual meson production (DVMP), specifically the reaction $\gamma^*p \rightarrow pM$, where M is a meson ($\pi, \eta, \rho, \omega, \phi, etc$). In the GPD approach, which is schematically shown in Fig. 1, the ingredients involve a hard interaction between a virtual photon and quark which produces a meson whose internal structure is given by the distribution amplitude $\Phi(z)$, and the remaining nucleon whose structure is

represented by GPDs. A caveat is that the proof for factorization applies only to the case when the virtual photon has longitudinal polarization. In that case, in the limit $Q^2 \rightarrow \infty$ the cross section scales as $\sigma_L \sim 1/Q^6$ and the ratio as $\sigma_T/\sigma_L \sim 1/Q^2$.

While most theoretical work on the GPD approach has focused on the high Q^2 and low $|t|$ kinematic region, exclusive production of photons and mesons at large $|t|$ can also be described in terms of the nucleon GPDs. Theory also predicts σ_L and σ_T in the high $-t$ low Q^2 region. For example for the pseudoscalar meson electroproduction we have:

$$\frac{d\sigma}{dt} \propto \left(R(t) \int dz \Phi(z) f(z, s, Q^2, t) \right)^2 \quad (1)$$

$$R(t) \propto (e_u R^u(t) - e_d R^d(t)^d) \quad R^q(t) = \int \frac{dx}{x} e^{\alpha t((1-x)/2x)} [\Delta q(x) - \Delta \bar{q}(x)]$$

where $\Phi(z)$ is the meson distribution amplitude, $f(z, s, Q^2, t)$ is parton level amplitude and the $R(t)$ s describe new form factors which are the $1/x$ moments of the GPDs. Δq and $\Delta \bar{q}$ are the polarized parton and antiparton distributions for u, d and s quarks. The constant in the exponent α is approximately 1 GeV^{-2} . The Fourier transforms with respect to $\vec{\Delta}_\perp$ ($\Delta^2 = -t$) describe the correlation between the transverse spatial distribution of quark impact and x_B in the proton.

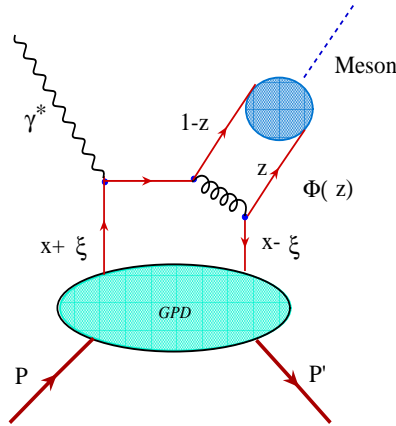


Figure 1. Schematic illustration of the GPD approach to meson electroproduction.

Deeply virtual Compton scattering (DVCS) is the cleanest way of accessing GPDs. However, DVCS does not allow to discriminate the helicity dependent GPDs and it is difficult to perform a flavor separation. In the case of pseudoscalar meson production the amplitude involves the axial vector-type GPDs \tilde{H} and \tilde{E} . These GPDs are closely related to the distribution of quark spin in the proton, and \tilde{H} reduces to the polarized quark/antiquark densities in the limit of zero momentum transfer. Vector and pseudoscalar meson production allows one to separate flavor and isolate the helicity-dependent GPDs. This is summarized in Table 1.

\tilde{H}, \tilde{E}	π^+	$\Delta u - \Delta d$
	π^0	$2\Delta u + \Delta d$
	η	$2\Delta u - \Delta d$
H, E	ρ^+	$u - d$
	ρ^0	$2u + d$
	ω	$2u - d$

The extraction of GPDs from electroproduction data is a challenging problem. A detailed understanding of the reaction mechanism is essential before one can compare with theoretical calculations. It is not yet clear at what values of Q^2 the application of GPDs to meson electroproduction becomes valid. However, detailed measurements of observables may test model-independent features of the reaction mechanism, such as t -slopes, flavor ratios, and generally by studying the variation of observables over a wide range of Q^2 and t . Even though current experiments are limited in Q^2 and t , it has been argued [2] that *precocious factorization* ratios of cross sections as a function of x_B could be valid at relatively lower Q^2 than for cross sections themselves. For example, the ratio of cross sections for π^0 and η electroproduction from a proton is related to the helicity structure of the quark flavors as

$$\pi^0/\eta = \frac{1}{2} \left[\frac{2}{3}\Delta u + \frac{1}{3}\Delta d \right]^2 / \frac{1}{6} \left[\frac{2}{3}\Delta u - \frac{1}{3}\Delta d + \frac{1}{3}\Delta s \right]^2 \quad (2)$$

The results of a calculation of this ratio as a function of x_B is shown in Fig. 2.

Recent CLAS measurements of π^0 and η production.

The beam spin asymmetries for DVCS [3] and DVMP [4] have recently been obtained at Jefferson Lab with the CLAS spectrometer, up to a $Q^2 \sim 5$

GeV² (see also previous CLAS publications [5] and [6]). This has been made possible by constructing a high quality electromagnetic calorimeter consisting of 424 lead-tungsten crystals covering an angular range from 4.5° to 15°, which was positioned into the existing CLAS large acceptance detector. The pions and etas are identified through their 2 γ decays. A photograph of the new detector and the 2 γ invariant mass distribution is shown in Fig. 3. One can see that the pions and etas are clearly observed, even before all final data selection cuts are performed. The kinematic coverage in the variables Q^2 , x_B , t and W is shown in Fig. 4.

The virtual photon cross section can be written in well known notation as

$$\frac{d\sigma}{d\Omega_\pi} = \sigma_T + \epsilon\sigma_L + \epsilon\sigma_{TT}\cos 2\phi + \sqrt{2\epsilon(1+\epsilon)}/2\sigma_{LT}\cos\phi_\pi + h\sqrt{\epsilon(\epsilon-1)}\sigma'_{LT}\sin\phi \quad (3)$$

where ϕ denotes the azimuthal angle between the hadronic and leptonic scattering planes and h is the electron beam polarization.

The large acceptance of CLAS enabled the data to be grouped into

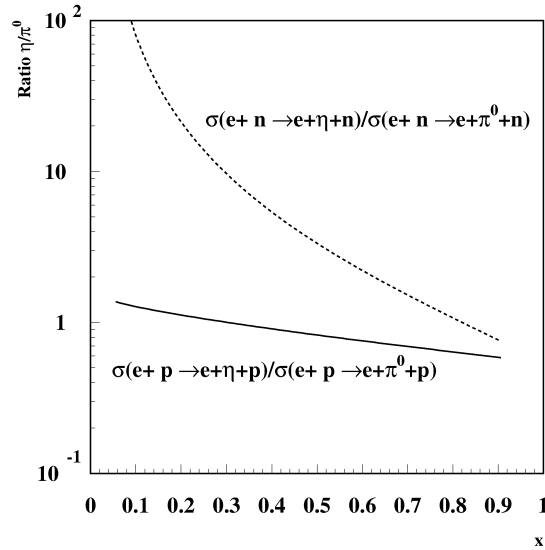


Figure 2. Predictions of the ratio of cross sections for π^0 to η electroproduction from protons and neutrons [2] utilizing the concept of *precocious factorization*.

intervals in Q^2 , t , x_B and ϕ . For unpolarized electrons ($h = 0$) the separation of the ϕ dependence in moments of a *constant*, $\cos\phi$, and $\cos 2\phi$ allows us to

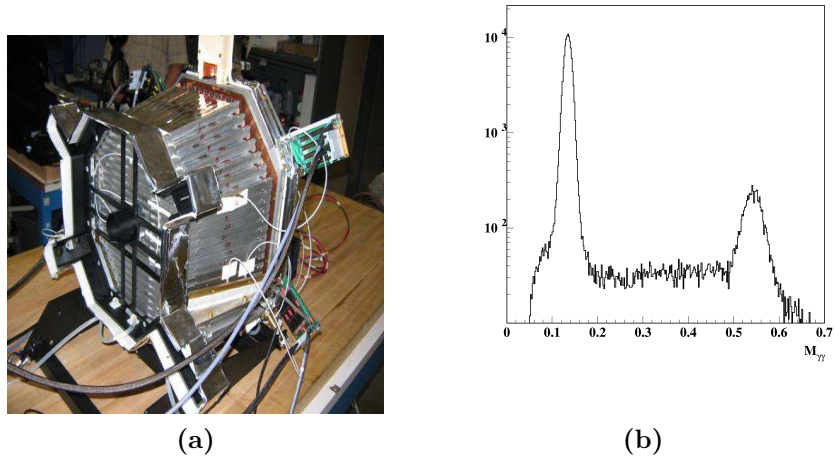


Figure 3a. Photograph of the new CLAS lead-tungsten electromagnetic calorimeter.

Figure 3b. 2γ invariant mass spectrum in which the π^0 's and η 's are clearly observed (note log scale).

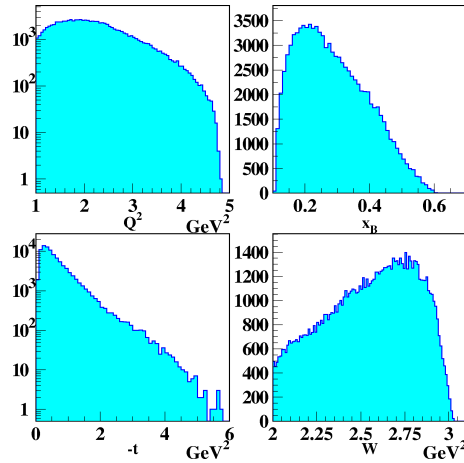


Figure 4. The kinematic coverage in Q^2 , t , x_B and W for neutral pions of the CLAS DVMP experiment.

obtain $\sigma_T + \epsilon\sigma_L$, σ_{TT} and σ_{LT} . An example of a ϕ distribution for $t = 0.3$ GeV^2 integrated over Q^2 are shown in Fig. 5.

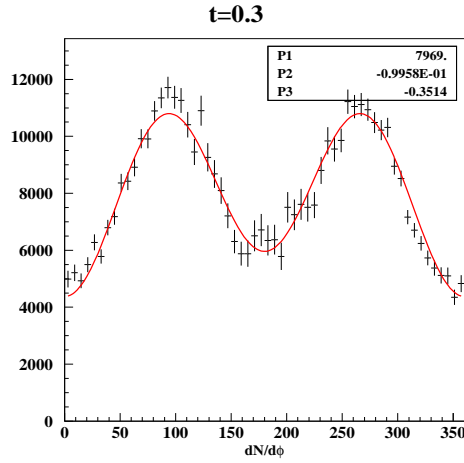


Figure 5. The angular distribution for $t = 0.3 \text{ GeV}^2$ integrated over $Q^2 > 1 \text{ GeV}^2$ and $W > 2 \text{ GeV}$.

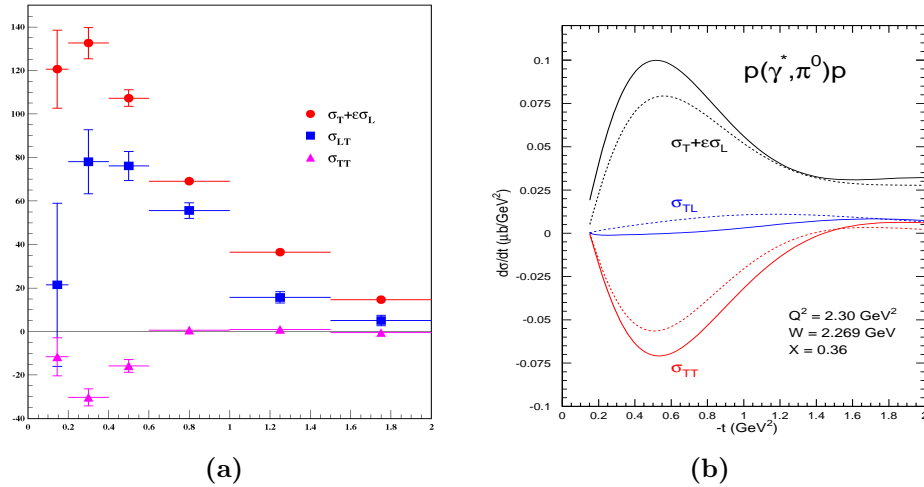


Figure 6a. The separated structure functions $\sigma_T + \epsilon\sigma_L$, σ_{TT} and σ_{LT} as a function of $-t$ at $Q^2 = 2.3 \text{ GeV}^2$ obtained with the CLAS spectrometer (very preliminary, arbitrary units).

Figure 6b. The results of a Regge model calculation [7].

The separated structure functions versus t for $Q^2 = 2.3 \text{ GeV}^2$ are shown in Fig. 6. The cross sections are in arbitrary units and radiative corrections have not been applied. It is observed that all the structure functions have significant non-zero values. σ_{LT} is comparable to $\sigma_T + \epsilon\sigma_L$ which implies that there are significant contributions of transverse amplitudes at these relatively low values of Q^2 , so the factorization cannot be applied. However, one may analyze these data in terms of a hadron based models such as Regge phenomenology [7]. Fig. 6 shows the results of such a calculation, which qualitatively follows the sign of the separated structure functions, but not always the shape.

The Fourier transformation of the GPDs gives information about the impact parameter \vec{b}_\perp dependence of parton distributions. The Fourier transformations are given by

$$F(x, \vec{b}_\perp) \propto \int \frac{d^2\vec{\Delta}_\perp}{2\pi} e^{i\vec{\Delta}_\perp \vec{b}_\perp} \tilde{H}(x, 0, \Delta_\perp^2) \quad (4)$$

Due to the significant contribution of transverse amplitudes at the current kinematics we do not have access to GPDs. However, we can apply a Fourier transformation to the cross sections to get impact parameter

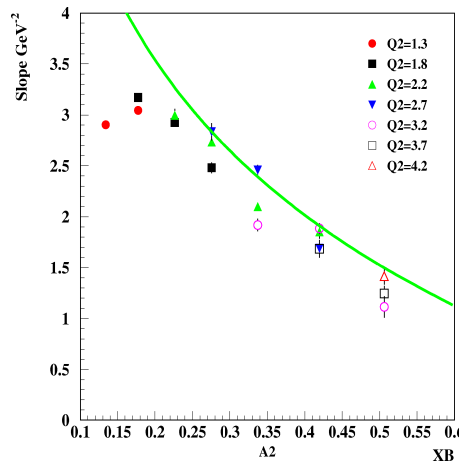


Figure 7. The experimental slope parameters B (very preliminary) obtained from fits to the data for various values of Q^2 and x_B with the function $d\sigma/dt \propto \exp(B(x_B, Q^2)t)$. The solid curve is the Regge inspired parametrization $B(x_B) = 2\alpha \ln(1/x_B)$ with $\alpha = 1.1$.

information. Slope parameters B have been extracted by fitting the t distributions using the parametrization $d\sigma/dt \propto \exp(B(x_B, Q^2)t)$. The result is shown in Fig. 7. Note that B does not appear to significantly depend on Q^2 .

In a Regge inspired GPD model, the x_B dependence of the slope parameter is given by $B(x_B) = 2\alpha \ln(1/x_B)$, with $\alpha \sim 1$ [8]. The curve in Fig. 7 is a plot of this parametrization for B . Remarkably, this curve appears to accurately account for the data with no further parameters or normalization applied.

For the interpretation in terms of the impact parameter, the Δ_{\perp}^2 slope is relevant, where Δ_{\perp}^2 is the transverse component of the momentum transfer ($\Delta^2 = t$), and the slope parameter is $B_{\perp} = \frac{B}{1-x_b}$ [9]. The fact that the t -slope goes to zero for large x_B may be purely kinematical. However, even taking into account this factor, we note that B_{\perp} falls with x_B in the region x_B from 0.1 to 0.5 where we have experimental data. This implies that the impact parameter distribution is broadest at lowest x_B and becomes narrower at increasing x_B .

The ratio of cross sections for η and π^0 .

As it was noted in the introduction the ratio of cross sections may play an important role due to the *precocious factorization*. This ratio is presented in Fig. 8 for the different values of t and Q^2 as a function of x_B . Note that this ratio is almost independent of x_B and varies from 0.3 to 0.4 with increasing t . This is in contrast with the prediction [2] (see Fig. 2), where this ratio is equal to 1. However, we can not compare directly with [2] since σ_L and σ_T were not separated.

Beam spin asymmetry.

The beam spin asymmetry (BSA) is defined by

$$A = \frac{\vec{\sigma} - \overleftarrow{\sigma}}{\vec{\sigma} + \overleftarrow{\sigma}} \sim \alpha \sin\phi. \quad (5)$$

From Eq. 3 the beam spin asymmetry directly yields the $L - T$ interference structure function σ'_{LT} . Any observation of a non-zero BSA would be indicative of an L-T interference. If σ_L dominates, then σ_{LT}, σ_{TT} , and σ'_{LT} should be small. An example of a ϕ distribution of the BSA for π^0 and η production at a particular kinematic bin is shown in Fig. 9.

Sizable beam-spin asymmetries for exclusive π^0 and η mesons electro-production have been measured above the resonance region for the first

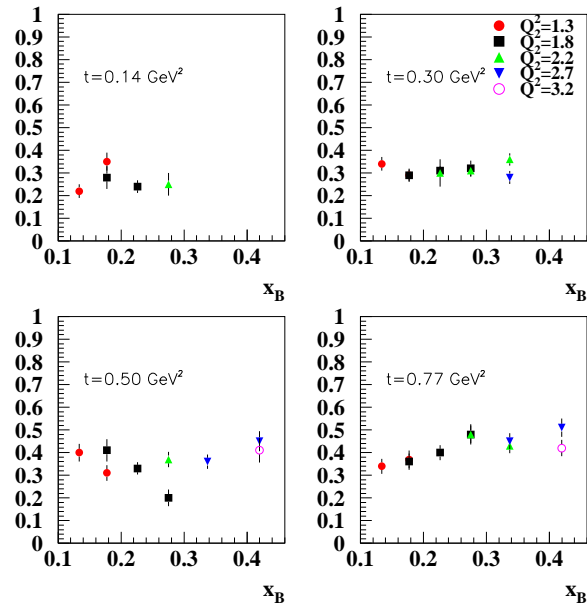


Figure 8. η to π^0 cross sections ratio as a function of x_B for different values of Q^2 and t (very preliminary).

time. These non-zero asymmetries imply that both transverse and longitudinal amplitudes participate in the process. However, the results of a Regge model calculation qualitatively describe the experimental data too.

Conclusion.

Cross sections and asymmetries for the π^0 and η exclusive electroproduction in a very wide kinematic range of Q^2 , t and x_B have been measured and initial analyses already are showing remarkable results. These data will help us to better understand the transition from soft to hard mechanisms. Initial results show that both transverse and longitudinal amplitudes participate in the exclusive processes at currently accessible kinematics. The π^0/η cross section ratio will check the hypothesis of precocious scaling.

We view the work presented here as leading into the program of the

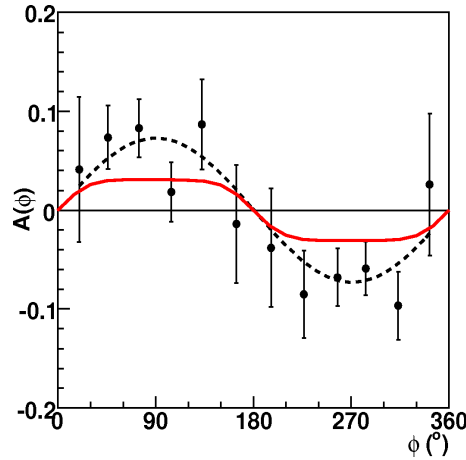


Figure 9. The angular distribution of the BSA for π^0 at $Q^2 = 2 \text{ GeV}^2$, $t = -0.3 \text{ GeV}^2$, and $x_B = 0.25$. The dashed curve is a fit to the function $A = \alpha \sin \phi$ and the solid curve is the result of a Regge model [7] calculation.

Jefferson Lab 12 GeV upgrade. The increased energy and luminosity will allow us to make the analysis presented here at much higher Q^2 and x_B as well as to perform Rosenbluth L/T separations. In parallel, we pose the following theoretical questions. What does the t -slope $B(Q^2, x_B)$ tell us? What can we learn from the Q^2 evolution of the cross sections? Can the measurement of σ_L , σ_T , σ_{LT} , σ_{TT} and $R \equiv \sigma_L/\sigma_T$ constrain GPDs within the approximations and corrections which have to be made due to non-asymptotic kinematics? How big are the corrections?

We acknowledge the outstanding efforts of the staff of the Accelerator and Physics Divisions at Jefferson Lab that made this experiment possible. We also acknowledge useful discussions with H. Avakian, M. Burkardt, V. Burkert, R. De Masi, M. Garcon, F-X Girod, G. Goldstein, L. Elouadrhiri, J-M. Laget, S. Liuti, S. Niccolai, R. Niyazov, S. Stepanyan, M. Strikman, A. Radyushkin, I. Strakovski, C. Weiss, and B. Zhao. This work was supported by the U.S. Department of Energy and National Science Foundation. The Jefferson Science Associates (JSA) operates the Thomas Jefferson National Accelerator Facility for the United States Department of Energy under contract DE-AC05-06OR23177.

References

1. J. C. Collins, L. Frankfurt and M. Strikman, Phys. Rev. D **56**, 2982, 1997.

2. M. I. Eides, L. L. Frankfurt and M. I. Strikman, Phys. Rev. D **59**, 114025, 1999.
3. CLAS collaboration, F.X. Girod et al., arXiv:0711.4805 [hep-ph], 29 Nov. 2007.
4. CLAS collaboration, R. De Masi et al., arXiv:0711.4736 [hep-ex], 4 Dec. 2007.
5. CLAS collaboration, S. Stepanyan et al., Phys. Rev. Lett.87:182002,2001.
6. CLAS collaboration, S. Chen et al., Phys. Rev. Lett.97:072002,2006.
7. J-M. Laget, private communication.
8. A.V. Belitsky, A.V. Radyushkin, Phys. Rept. 418, 1-387, 2005.
9. Mattias Burkardt, arXiv:0711.1881 [hep-ph], 13 Nov. 2007.